STIMULATED RAMAN SCATTERING IN ARAGONITE

B. M. ATAEV

P. N. Lebedev Physics Institute, USSR Academy of Sciences

Submitted June 5, 1969

Zh. Eksp. Teor. Fiz. 57, 1551–1554 (November, 1969)

Stimulated Raman scattering with a vibrational transition frequency $\omega_0 = 1086\ cm^{-1}$ is observed in a biaxial crystal of aragonite ($CaCO_3$). Emission of four anti-Stokes and two Stokes components is observed. The angular distribution of the four anti-Stokes and of the second Stokes components is measured. The emission angles of the four anti-Stokes components in aragonite are evaluated on the basis of the theory of Raman scattering of light developed by Lugovoĭ. Good agreement between the calculated and measured values of the angles is found.

THIS paper reports the results of an investigation of the angular distribution of the components of stimulated Raman scattering (SRS) in a biaxial crystal of aragonite ($CaCO_3$). The pattern of radiation in definite cones was obtained for the four anti-Stokes and the second Stokes components. Since the refractive index of aragonite is known, it was found possible to predict the position of the anti-Stokes components on the basis of the theory developed by Lugovoĭ[1] and to compare the results of the calculation with the experimental data.

According to[1], the equation for the emission angles of the anti-Stokes components in biaxial crystals $\vartheta_m^{\alpha\beta\gamma}$ has the following form:

$$(\vartheta_m^{\alpha\beta\gamma})^2=(\vartheta_m^{(0)})^2-Q(p)\frac{mk_{-1}}{(m+1)k_0}\Big\{(-1)^\beta[(\vartheta_m^{\alpha\beta\gamma})^2+\psi^2-2\vartheta_m^{\alpha\beta\gamma}\psi\cos\varphi]^{1/2}$$
$$+(-1)^\alpha\Big[(\vartheta_m^{\alpha\beta\gamma})^2+\Big(\frac{mk_{-1}}{k_m}\psi\Big)^2+2\frac{mk_{-1}}{k_m}\psi\vartheta_m^{\alpha\beta\gamma}\cos\varphi\Big]^{1/2}\Big\}$$
$$+(-1)^\gamma Q(p)\frac{mk_{-1}}{k_m}\psi. \qquad (1)$$

where

$$\vartheta_m^{(0)}=\Big[-\frac{2mK_{-1}^{(0)}[K_m^{(0)}+mK_{-1}^{(0)}-(m+1)K_0^{(0)}]}{(m+1)K_0^{(0)}K_m^{(0)}}\Big]^{1/2}, \qquad (2)$$

$$Q=\Big[\frac{(\varepsilon^{(z)}-\varepsilon^{(y)})(\varepsilon^{(y)}-\varepsilon^{(x)})}{\varepsilon^{(x)}\varepsilon^{(z)}}\Big]^{1/2}, \qquad (3)$$

$$\varepsilon^{(x)}<\varepsilon^{(y)}<\varepsilon^{(z)},\quad K_m^{(0)}=k_m\sqrt{\varepsilon^{(y)}(\omega_m)},\quad k_m=\omega_m/c,\quad k_0=p/c,$$

p is the frequency of the pump wave, ψ is the angle between the direction of one of the optic axes of the crystal and the wave vector $\mathbf{K}_{0\gamma}$ of the pump wave, φ is the angle between the plane passing through the scattering point, the wave vector $\mathbf{K}_{0\gamma}$, and the optic axis, and the plane passing through the same vector and the wave vector $\mathbf{K}_{m\beta}$ of the scattered component under consideration. The quantity $\vartheta_m^{(0)}$ is the angle which would be observed in an isotropic medium with refractive index $n(\omega) = [\epsilon^{(y)}(\omega)]^{1/2}$. Equation (1), which determines the real positive roots for $\vartheta_m^{\alpha\beta\gamma}$, is an algebraic equation of the eighth degree depending on the parameter φ. The solution is difficult in the general case. However, in the special case when the pump wave vector is directed along an optic axis of the crystal ($\psi = 0$), the corresponding solution obtained in[1] is

$$\vartheta_m^{\alpha\beta\gamma}=-\frac{Qmk_{-1}}{2(m+1)k_0}[(-1)^\alpha+(-1)^\beta]$$
$$+\Big\{\Big(\frac{Qmk_{-1}}{2(m+1)k_0}\Big)^2[(-1)^\alpha+(-1)^\beta]^2+(\vartheta_m^{(0)})^2\Big\}^{1/2}.$$

Equation (4) defines circular cones of emission of the anti-Stokes components, the axes of which pass through the scattering point parallel to the vector $\mathbf{K}_{0\gamma}$ and which have vertex angles equal to $2\vartheta_m^{\alpha\beta\gamma}$. The intersections of these cones with a plane perpendicular to the wave vector $\mathbf{K}_{0\gamma}$ beyond the scattering point are concentric circles. Of course, for sufficiently small ψ Eq. (1) will define anti-Stokes cones whose intersections with this plane are nearly cicrles. An increase in ψ ($\psi > 1°$) leads to emission of the anti-Stokes components along conical surfaces that may be of more complex form than circular cones. Correspondingly, the intersections of these surfaces with the perpendicular plane will be more complex curves than circles.

In our experiments, the sharpest pattern of the angular distribution of the anti-Stokes components was observed in the direction of the intersection of the plane of the optic axes with the corresponding cones. Hence it was convenient to compare the distances from the center of the pump beam to the points of intersection of the plane of the optic axes with the anti-Stokes cones. This direction corresponds to $\varphi = \pi$. In this case, one obtains from Eq. (1) the following expression for the angles ϑ_m^{222} of the fundamental emission ($\alpha = \beta = 2$) of the anti-Stokes components:

$$\vartheta_m^{222}=-Q\frac{mK_{-1}}{(m+1)K_0}+\Big[\Big(\frac{QmK_{-1}}{(m+1)K_0}\Big)^2+(\vartheta_m^{(0)})^2+\psi\frac{2QmK_{-1}}{(m+1)K_0}\Big]^{1/2}. \qquad (5)$$

According to this relation, the angles ϑ_m^{222} depend on ψ. As ψ increases, so do the corresponding angles ϑ_m^{222}. At the same time the angles ϑ_m^{122} of the supplementary anti-Stokes emission ($\alpha = 1$, $\beta = 2$) for $\varphi = \pi$ do not depend on ψ. In the special case when the wave vector of the pump is directed along an optic axis ($\psi = 0$), Eq. (5) reduces to Eq. (4). The situation is analogous for the higher Stokes components.[1]

For a numerical calculation of the angles $\vartheta_m^{\alpha\beta\gamma}$ for $\varphi = \pi$ we used the data on the refractive index of aragonite given in[2]; the frequency of the transition $\omega_0 = 1086\ cm^{-1}$ corresponds to completely symmetrical vibrations of the CO_3^{--} ions,[3] and the frequency of the incident wave is the frequency of a ruby laser. The values of the refractive indices for the necessary wave

lengths λ_m were obtained from approximations of the functions $n(\lambda)$ according to the values given in[2]. The curve $n_\beta(\lambda)$ was approximated by a polynomial of third degree in λ, which gives an accuracy of $\pm 10^{-5}$. Using the values of the refractive indices obtained in this way, we find from Eq. (3) $Q = 3.25778 \times 10^{-2}$. The dependence of the angle between the optic axes on wavelength $2V(\lambda)$ is given in[2]. The effect of the dispersion of this angle on the emission angles of the components is not large; for example, for the fourth anti-Stokes component it amounts to $\sim 0.76 \times 10^{-3}$ rad.

In the experiments we used a sample of single-crystal aragonite of length 16 mm, cut perpendicular to one of the optic axes. The sample was oriented so that the electric vector of the exciting radiation was perpendicular to the plane of the optic axes and the laser beam passed through the crystal as if through a medium with refractive index $n = [\epsilon^{(y)}(\omega)]^{1/2}$. The power of the exciting ruby laser with Q switching (rotating prism) was 30 MW for a pulse length of 25 nsec. The laser beam was converged by a lens with f = 30 cm. The distance from the exit face of the sample to the focus of the lens was about 7 cm. The aragonite crystal was vibrated in the plane of the optic axes over an interval of 10′ both toward the side of decreasing angle between the direction of the pump beam and the direction of the biradial and toward the other side. In doing this, the angle ψ between the beam direction and the given optic axis varied from 0 to about 3°. The scattered radiation, after filtration to attenuate the pump radiation, fell directly on a photographic film. The radiation of the anti-Stokes components was isolated with the aid of SZS-15 and SZS-21 filters. To this end, we also used a liquid filter of $CuSO_4$ solution. Photographs of the Stokes components of second order were obtained on INFRA-850 infrared film in combination with SS-4 and FS-7 filters. In this way, we were able to obtain rather sharp patterns of the fundamental and supplementary emissions of the four anti-Stokes and the second Stokes components.

Figure 1 shows a typical photograph of the angular distribution of the anti-Stokes components characteristic for a change in ψ from 10′ to 45′ (the crystal was vibrated toward the side of decreasing angle between the beam direction and the biradial). Measurement of the distances from the center of the spot due to the pump

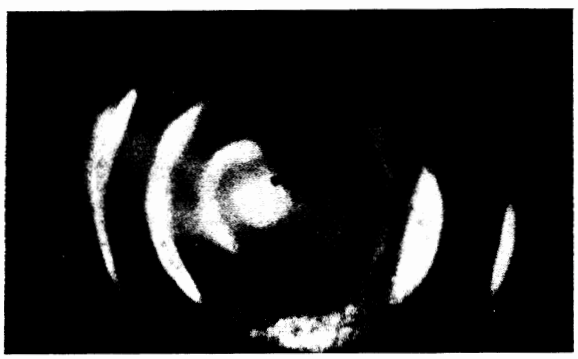

FIG. 1. Radiation pattern of anti-Stokes components of SRS in aragonite, observed at $\psi = 0.58 \times 10^{-2}$ rad. To the left of the laser spot are the half-rings of the fundamental emission of the four anti-Stokes components; to the right appears the supplementary emission of the same components.

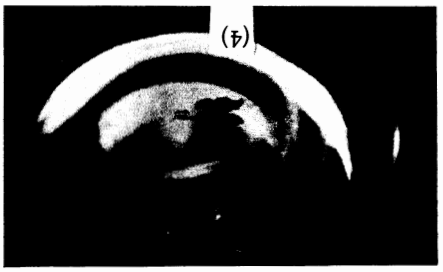

FIG. 2. Radiation pattern of anti-Stokes components of SRS in aragonite, observed at $\psi = 2.62 \times 10^{-2}$ rad.

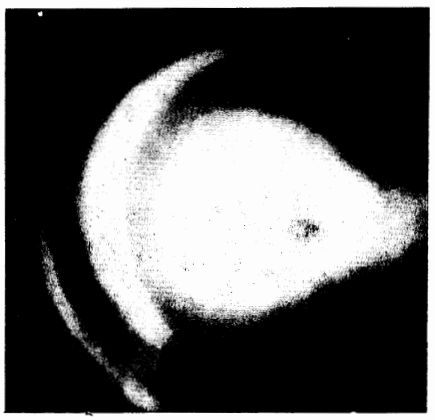

FIG. 3. Radiation pattern of Stokes components of SRS in aragonite, observed at $\psi = 0.29 \times 10^{-2}$ rad. Visible are the rings of emission of the second Stokes component, as well the spot of diffuse radiation of the first Stokes component with maximum intensity in the direction of the pump beam.

to the corresponding components in the direction of the intersection of the plane of the optic axes with the film showed that within this range of ψ, the angles of the supplementary radiation ϑ_m^{122} do not depend on ψ. The angles of the fundamental radiation ϑ_m^{222} do depend on ψ. As ψ increases, the distances from the center of the pump spot to the corresponding emission of the fundamental components also increases. Upon further increase in ψ ($\psi > 1°$) both the fundamental and supplementary emissions of the anti-Stokes components, in agreement with theory, go along conic surfaces more complex than circular, and one sees more complex curves than circles on the film (see Fig. 2). The same pattern is observed also when the orientation of the crystal is deflected toward the side of increasing angle between the pump beam direction and the biradial, just as in the case when it is deflected outside of the plane of the optic axes.

In Fig. 3 is shown the typical pattern of emission of the Stokes components for a change in ψ of from 10′ to 45′. In the immediate vicinity of the optic axis ($\psi = 0$), we were unable to obtain a sufficiently sharp pattern of the emission for both the Stokes and anti-Stokes components. A possible explanation for this is the presence of internal conical refraction of the laser beam in directions close to an optic axis of the crystal. The measured values of the angles ϑ_m^{122} of the supplementary radiation of the four anti-Stokes and the second Stokes components, as well as the calculated values of the same angles for the four anti-Stokes components, are presented in Table I.

Table I. Values of ϑ_m^{122} (in units of 10^{-2} rad)

Frequency	Wavelength, Å	Experiment: Measured with lens f = 30 cm	Experiment: Extrapolation to f = ∞	Theory
$p-2\omega_0$	8175.4	3.80	3.41	—
$p+\omega_0$	6455.8	2.35	1.96	1.96
$p+2\omega_0$	6032.8	4.71	4.32	4.35
$p+3\omega_0$	5661.9	7.05	6.66	6.59
$p+4\omega_0$	5333.9	9.35	8.96	8.83

Here it should be kept in mind that under the conditions of the experiment, the pump beam inside the crystal is not strictly parallel. The angles observed under similar conditions are found to be somewhat larger than those calculated for a parallel beam (see, for example,[4,5]). It turned out that an extrapolation of the results obtained with the lens with f = 30 cm to f = ∞ leads to a decrease in the emission angles of all components of almost exactly the same amount (0.39×10^{-2} rad). Apparently, this is because convergence of the pump beam leads to an increase in the angles at the moment of eruption of all the components from the active region. Together with the measured values obtained with the lens with f = 30 cm, we also give the values obtained by extrapolation to f = ∞.

Table II presents the dependence of the angles of the fundamental anti-Stokes radiation ϑ_m^{222} on ψ within the limits of variation of ψ from 10′ to 45′. The calculated values of these angles for the indicated values of ψ, obtained from Eq. (4), are also given there. Tables I and II show a good agreement between the measured quantities and those calculated from Lugovoĭ's theory.[1]

Table II. Values of ϑ_m^{222} (in units of 10^{-2} rad)

Frequency	ψ = 10′			ψ = 20′			ψ = 30′			ψ = 45′		
	Experiment		Theory	Experiment		Theory	Experiment		Theory	Experiment		Theory
	f = 30 cm	f = ∞		f = 30 cm	f = ∞		f = 30 cm	f = ∞		f = 30 cm	f = ∞	
$p+\omega_0$	1.30	0.91	0.89	1.50	1.11	1.09	1.68	1.29	1.29	1.93	1.59	1.57
$p+2\omega_0$	2.70	2.31	2.23	2.81	2.42	2.40	3.05	2.66	2.53	3.35	2.96	2.89
$p+3\omega_0$	4.37	3.98	3.91	4.45	4.06	4.10	4.70	4.31	4.25	—	—	—
$p+4\omega_0$	6.20	5.81	5.82	6.34	5.95	5.94	6.54	6.15	6.06	—	—	—
$p-\omega_0$	5.18	4.79	—	—	—	—	—	—	—	—	—	—

In conclusion, I thank Acad. A. M. Prokhorov and F. V. Bunkin for their attention and support, and V. N. Lugovoĭ for helpful discussions and stimulation. I am also grateful to Z. A. Magomedov for the aragonite crystal.

[1] V. N. Lugovoĭ, Vvedenie v teoriyu vynuzhdennogo kombinatsionnogo rasseyaniya (Introduction to the Theory of Stimulated Raman Scattering), Nauka, 1968.

[2] Landolt-Börnstein, Zahlenwerte und Funktionen, Bd. 1, T. 2, Berlin, 1923.

[3] K. W. F. Kohlrausch, Ramanspektren, Akademische Verlag, Leipzig, 1943 (Russ. Transl., IIL, 1952, p. 359).

[4] R. Chiao and B. P. Stoicheff, Phys. Ref. Lett. 12, 290 (1964).

[5] B. M. Ataev and V. N. Lugovoĭ, Fiz. Tverd. Tela 10, 1991 (1968) [Sov. Phys.-Solid State 10, 1566 (1969)].

Translated by L. M. Matarrese
181